Materials Transactions, Vol. 61, No. 4 (2020) pp. 562 to 566
Special Issue on Materials Science on High-Entropy Alloys

Microstructure and Mechanical Behavior of Ti–25Nb–25Zr Alloy Prepared from Pre-Alloyed and Hydride-Mixed Elemental Powders

Bhupendra Sharma[1,*], Sanjay Kumar Vajpai[2], Mie Kawabata[3], Takayoshi Nakano[4] and Kei Ameyama[3]

[1]*Research Organization of Science and Technology, Ritsumeikan University, Kusatsu 525-8577, Japan*
[2]*Department of Metallurgical and Materials Engineering, National Institute of Technology, Jamshedpur, India*
[3]*Faculty of Science and Engineering, Ritsumeikan University, Kusatsu 525-8577, Japan*
[4]*Division of Materials and Manufacturing Science, Graduate School of Engineering, Osaka University, Suita 565-0871, Japan*

A study has been undertaken on the feasibility of the powder-metallurgy manufacturing process to fabricate β-type Ti–25Nb–25Zr alloy (mass%) for biomedical applications. The Ti–25Nb–25Zr alloy was fabricated from a mixture of TiH_2 with constituent elemental powders, and from a pre-alloyed Plasma Rotating Electrode Processed (PREP) Ti–25Nb–25Zr powder, separately. It is shown that different processing methods led to different microstructures and mechanical properties. The Ti–25Nb–25Zr compact prepared by pre-alloyed powder exhibits poor strength whereas TiH_2 processed Ti–25Nb–25Zr compact exhibits comparatively ultra-fine grained microstructure with significantly improved strength. The proposed fabrication method may have several opportunities to fabricate metallic alloys with enhanced mechanical properties.
[doi:10.2320/matertrans.MT-MK2019001]

(Received September 5, 2019; Accepted January 15, 2020; Published March 2, 2020)

Keywords: *powder metallurgy, mechanical milling, spark plasma sintering, titanium hydride, low entropy Ti–Nb–Zr alloys*

1. Introduction

Titanium and its alloys are one of the most illustrious biomaterials in orthopedic and dentistry fields owing to their superior biocompatibility, and excellent mechanical properties. Commercially pure titanium (CP-Ti) and Ti-based alloys have been frequently utilized for hard tissue replacements. However, there are several possible health issues with conventionally used structural biomaterials, such as Al and V in Ti–6Al–4V alloy, and higher Young's modulus ($\sim$110 GPa) of CP-Ti as compared to that of the human bone ($\sim$30 GPa).[1–3] Therefore, the selection of optimized Ti alloys for implantation purposes is determined by a combination of favorable characteristics including immunity to corrosion, biocompatibility, osseointegration, and excellent strength to weight ratio, good fracture toughness, high fatigue strength and low Young's modulus.[4–6] Therefore, the new generations of low modulus β titanium alloys which are free from toxic elements are more preferable for biomedical implants. In particular, alloys containing nontoxic elements such as Ti, Nb, Zr, Sn, and Ta are being extensively evaluated since these elements have been identified as exhibiting no adverse effects under the human body environment.[7] In those aspects, a newly developed low entropy ($\Delta S_{conf} = 0.88R$) biomedical grade β Ti–25Nb–25Zr (Mass%) alloy can be considered as a prospective biomaterial due to its excellent biocompatibility, low Young's modulus, excellent corrosion resistance, high phase stability under both severe plastic deformation and annealing conditions.[8–13] However, the mechanical properties of Ti–Nb–Zr alloys are poor[14] when compared to the other structural biomaterials such as Ti–6Al–4V,[15] Co–Cr–Mo alloys.[16]

Mechanical properties are one of the important aspects of all structural materials, including biomedical implants for load-bearing applications. Out of these aspects, the processing route plays an important role in terms of its ability to provide viable technological capability to produce desired products with requisite microstructure. Particularly for structural biomaterials, the Powder Metallurgy (PM) processing technique is considered to be an effective way of reducing the higher machining costs of Ti alloys via producing near-net shape products. Furthermore, it has the advantage of producing a compositionally homogeneous alloy as compared to other techniques, especially when the alloying element has a higher melting temperature, such as Nb and Zr in Ti-based alloys.[17]

The PM process based on Mechanical Milling (MM) of a systematically optimized mixture of titanium hydride (TiH_2) and elemental powders followed by sintering via Spark Plasma Sintering (SPS) is a promising method of preparing commercially pure-Ti and binary β-Ti alloys with fine-grained microstructure and excellent mechanical properties.[18–20] It was demonstrated that the use of a balanced amount of brittle TiH_2 powder in the initial powder mixture was advantageous not only suppressing the problem of sticking and agglomeration of Ti powder during MM but also avoiding the contamination caused by use of organic process control agents. Furthermore, the use of TiH_2 powder provides an economic advantage and superior mechanical properties as compared to similar alloy prepared using pure-Ti.[21–25]

Therefore the objective of the present work is to evaluate the possibility of preparing Ti–25Nb–25Zr alloy from a mixture of TiH_2 and elemental powders based method as well from pre-alloyed powder and to investigate the effect of two different powder metallurgy methods on the microstructure and mechanical properties. The microstructure, phase composition, mechanical properties of the sintered compacts have been studied, and the results of the same are presented and discussed.

2. Materials and Methods

The Ti–25Nb–25Zr alloy compacts were prepared by MM

*Corresponding author, E-mail: bhupen@fc.ritsumei.ac.jp

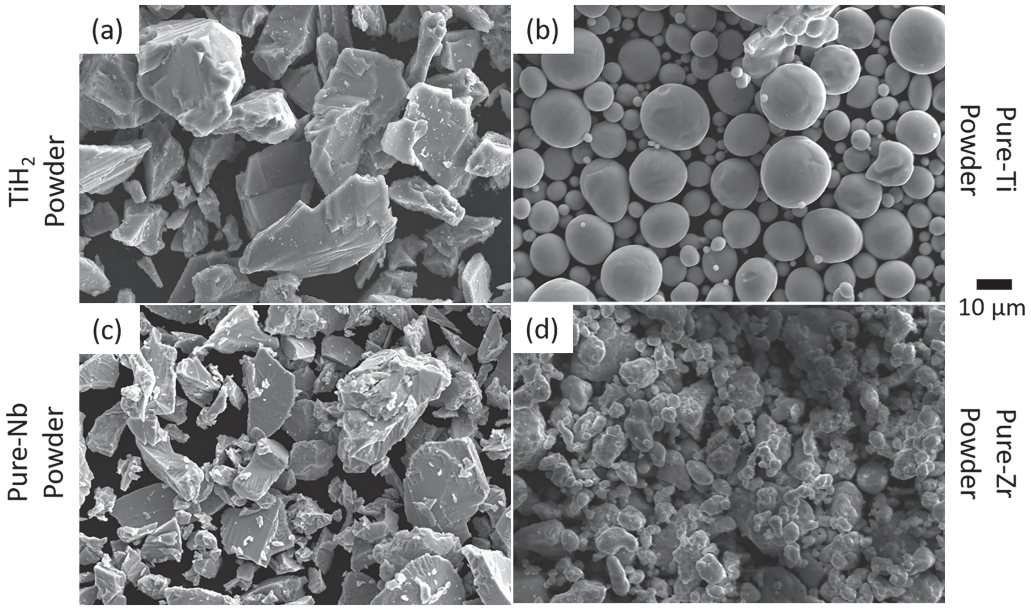

Fig. 1 The morphologies of as-received (a) TiH_2, (b) pure-Ti, (c) pure-Nb, and (d) pure-Zr powder particles.

Table 1 The processing parameters of Spark Plasma Sintering (SPS).

Heating/Cooling rate	100 K/Min
Holding Time	1.8 ks
Temperature	1273 K
Pressure	50 MPa

of a mixture of titanium hydride and elemental Ti, Nb, Zr powders (MM-Process). Figure 1 displays the morphology of as-received powders. For the comparison of microstructure and mechanical properties, similar alloy compacts were prepared by pre-alloyed plasma rotating electrode processed (PREP) Ti–25Nb–25Zr powder also (IP-Process).

In the MM-Process, as-received TiH_2, and pure-Ti, Nb, and Zr powders were mixed in an equal amount (i.e., 25 mass% each), under an argon atmosphere, and then subsequently sealed in stainless steel vial containing SUS balls. The amount of TiH_2 mixed with other elements and MM time was adjusted based on our previous work and the ball to powder ratio was maintained at 5:1 during MM.[20] The MM was carried out for 72 ks using a planetary ball mill operated at a constant speed of 200 rpm. During sintering, the MM powder was dehydrogenated at 1073 K for 7.2 ks in the SPS chamber while maintaining a high vacuum ($\sim 10^{-3}$ Pa) without applying any external load to minimize the amount of hydrogen content in the final bulk specimen. Subsequently, the dehydrogenated MM powder was sintered via SPS under the conditions mentioned in Table 1. The dehydrogenation and subsequent sintering process, in the SPS chamber, is referred to as a "two-step rapid-sintering process". The dehydrogenation temperature and two-step rapid-sintering SPS process were adjusted based on our previous study on commercially pure titanium (CP-Ti), wherein a good mechanical property was achieved for CP-Ti.[19] The mechanically milled powder and its corresponding sintered compact will be referred to as "MM-Powder" and "MM-Compact", respectively.

In the IP-Process, Ti–25Nb–25Zr compacts were fabricated from pre-alloyed PREP Ti–25Nb–25Zr powder (further referred to as "IP-Powder"). The IP-powder was sintered via SPS under the similar conditions mentioned in Table 1. The compact prepared by IP-Powder will be mentioned as "IP-Compact". IP-powder had an average particle size of approximately 220 μm.

In both MM-process and IP-process, the powder consolidation was carried out via Spark Plasma Sintering (Dr. Sinter, Sumitomo Coal Mining Co. Ltd., Japan) under high vacuum conditions ($\sim 10^{-3}$ Pa), using graphite die and punch. The disc-shaped compacts with dimensions 20×5 (mm^2) were obtained after the SPS process.

The phase analysis was performed by X-ray Diffraction (XRD) method using CuK_α ($\lambda = 1.5406$ Å) radiation. The microstructural characterization was carried out by Scanning Electron Microscope (SEM) equipped with Back Scattered Electron (BSE) and Electron Backscattered Diffraction (EBSD) facilities (step-size 0.1–2.3 μm). The primary elemental characterization was carried out by Energy Dispersive X-ray Spectroscopy (EDS). The grain size analysis was performed using the line intercept method on at least five images (~ 300 μm $\times$ 200 μm). EBSD data were processed in an HKL Channel 5 software package.

The mechanical properties of the specimens were analyzed by tension tests carried out at an initial strain rate of $5.6 \times 10^{-4}\ s^{-1}$ using specimens with gauge dimensions of $3 \times 1 \times 1$ (mm^3). At least three samples were considered to measure and calculate the average strength and elongation of as-fabricated Ti–25Nb–25Zr alloy.

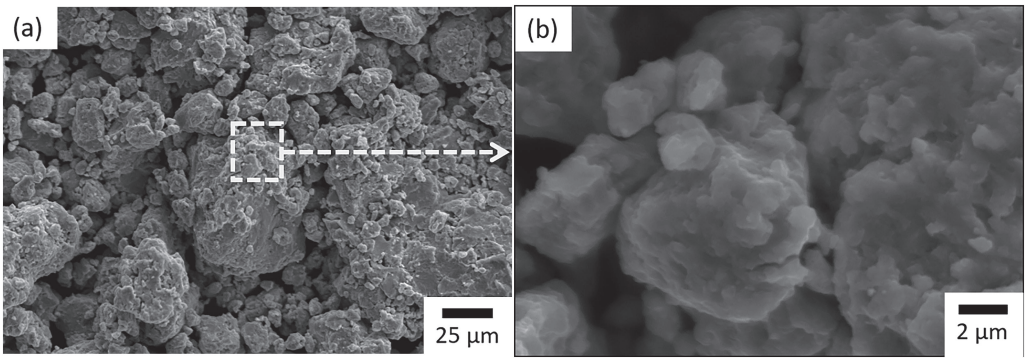

Fig. 2 SEM images of MM-Powder at (a) low and (b) high magnification scale.

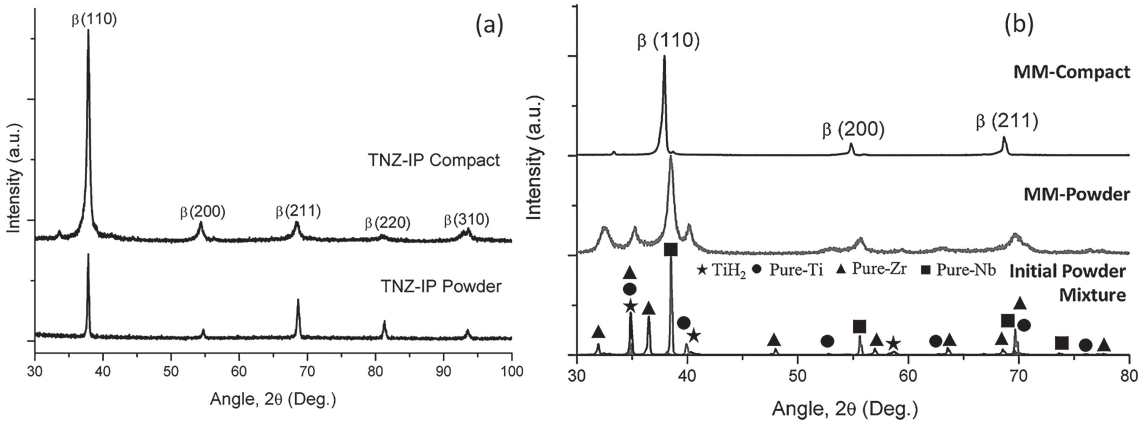

Fig. 3 The XRD patterns of (a) IP-Powder and IP-Compact, and (b) the mixture of as-received TiH_2 and elemental powders, MM-Powder, and MM-Compact.

3. Results and Discussion

The secondary electron (SE) images showing the morphology of the MM-Powder are presented in Fig. 2. It can be noticed that the shape of the powder particles is relatively spherical and more uniform as compared to that of the irregular shaped as-received powders (Fig. 1). Moreover, the coarser particles in the MM powder appear to be an agglomerate of fine particles of elements. The mean powder particle size of MM-powder was approximately 5 μm as obtained by particle size analysis. In comparison with initial powder particle sizes, it is clear that the average particle size after the MM process is significantly reduced.

The XRD pattern of the IP-Powder and IP-Compact (Fig. 3(a)) comprised of diffraction peaks of single β-phase that also confirmed the absence of any external impurities of oxidation. In contrast, no change in the position of the peak corresponding to the BCC phase was observed. The XRD results of a powder mixture of as-received TiH_2, pure-Ti, pure-Nb, pure-Zr powders, their 72 ks MM-Powder, and MM-Compact are shown in Fig. 3(b). The comparative analysis of the XRD patterns of a powder mixture of as-received powders (Fig. 3(a)) and MM-Powder (Fig. 3(b)) clearly indicates that the diffraction peaks are broadened and overlapped in MM-Powder which makes the interpretation of the pattern slightly cumbersome. However, an analysis of XRD patterns together with chemical analysis, by EDS, confirms that the significant broadening and intensity reduction in the XRD peaks corresponding to elemental powders can be attributed to the plastic deformation and fragmentation of large-sized particles into fine-size particles, during MM. Obviously, the mechanochemical reaction between brittle TiH_2 and ductile elemental powder particles (Pure Ti, Nb, and Zr), resulting in the partial hydrogenation of the highly activated surface of deformed elemental powder particles cannot be ruled out. The mechanism of such kind of particle fragmentation for ductile and brittle powder mixture has already been reported elsewhere.[18] Figure 3(b) shows the XRD results of MM-Compact, which indicates that the MM-Compact consisted of primarily β-phase. Also, the microstructural characterization confirmed the absence of other defects, such as residual porosity and/or chemical heterogeneity. Therefore, the XRD and SEM results suggested that the sintering at 1273 K led to the dissolution of Nb and Zr in the matrix, resulting in approximately complete β-phase.

In order to estimate the grain size, grain morphology, and phase constitution of the Ti–25Nb–25Zr compacts, the EBSD analysis was carried out. Figure 4 presents the EBSD image quality (IQ) map of the IP-Compact (Fig. 4(a)) and MM-Compact (Fig. 4(b)). It can be seen that both the IP-Compact and MM-Compact exhibit only homogeneous structured equiaxed types of microstructures. The equiaxed type of microstructure is a typical characteristic associated with the formation of β-type Ti alloys. However, the grain size is significantly different for both the compacts. The mean grain size for IP-Compact is $\sim 800 \pm 50$ μm whereas for MM-Compact it is 4.6 ± 2 μm.

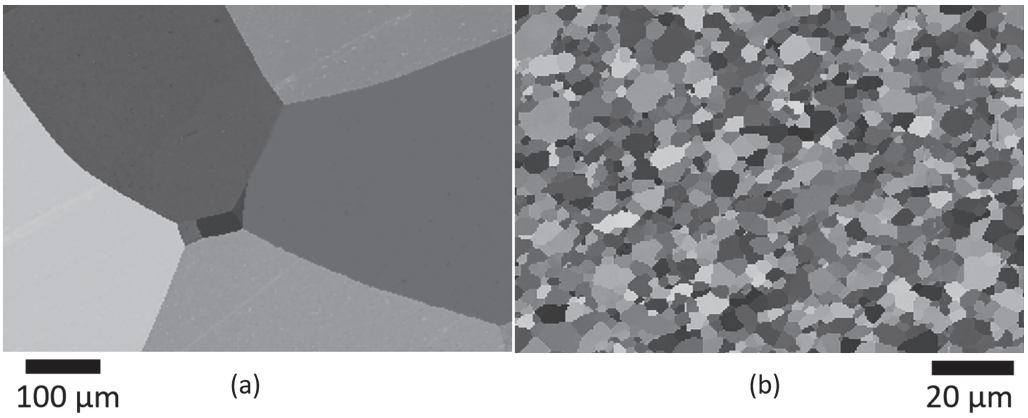

Fig. 4 EBSD micrographs of (a) IP-Compact and (b) MM-Compact.

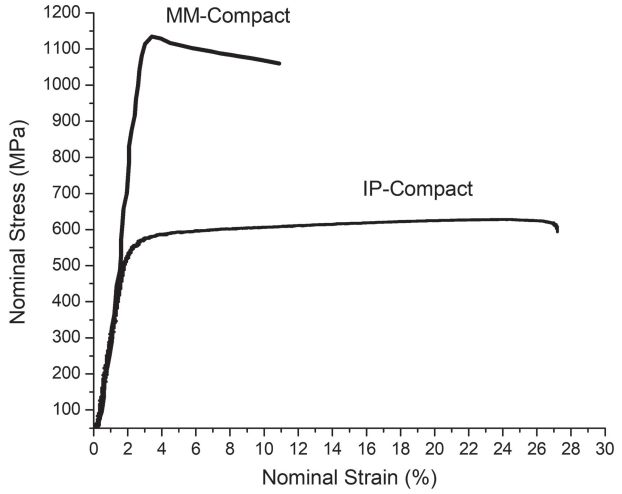

Fig. 5 Engineering stress-strain curves of IP-Compact MM-Compact.

In studies by Kohn *et al.*[26] and Morasch *et al.*,[27] it was presented that hydrogenation and dehydrogenation treatment of titanium alloys leads to the grain refinement and improvement in mechanical properties of β titanium alloys, wherein it was indicated that the grain refinement occurs due to the recrystallized grains originated from the titanium hydride. Therefore, fine grains for MM-Compact can be correlated with the use of titanium hydride as a temporary alloying element for processing with the elemental titanium, niobium, and zirconium powder mixture.

Figure 5 shows the representative stress-strain curves of both IP-Compact and MM-Compact. The tensile strength and elongation to fracture of IP-Compact are 631 ± 7 MPa and $27 \pm 15.3\%$ whereas for MM-Compact it is 1140 ± 13 MPa and $11 \pm 3\%$, respectively. However, IP-Compact exhibits uniform elongation whereas early necking was observed for MM-Compact. By contrast, the tensile strength of the MM-Compact is approximately 80% higher whereas elongation to fracture is approximately 60% lesser than that of the IP-Compact. While, the IP-Compact and MM-Compact both consist of equiaxed grains, higher strength and early necking of MM-Compact might be the result of relatively extremely finer microstructure obtained by the sintering of MM-Powder consisting of sub-micron sized powder particles. As can be observed from Fig. 5, the MM compact shows a limited plasticity in comparison with the IP-compact; if the plastic flow plateau (material flow at maximum load) is compared, it is a few times higher for the IP-compact comparing to the MM-compact, due to increased deformation capacity by slip/twinning of coarse-grained microstructure. However, it should be noted that despite a decrease of total elongation, it is still comparable to that of the other titanium-based structural biomaterials[14–16,28,29] and BCC type high entropy alloys.[30]

It has been reported that nanocrystalline materials possess higher surface energy and larger surface area than the coarse-grained materials which leads to enhanced interaction of implant surface with cells resulting in enhanced proliferation and cell attachment on the implant surface.[31,32] Therefore, the fine-grained Ti–25Nb–25Zr alloy is highly suited for biomedical applications as an implant in the orthopedic and dentistry field. By contrast, Ti–25Nb–25Zr alloy prepared by TiH_2 and elemental powders can be considered as a more favorable specimen, as a biomaterial, in terms of cost-effective process, stable β phase, fine grain microstructure and high tensile strength with acceptable ductility.

4. Conclusions

An investigation was carried out on the role of starting powder conditions, in the powder metallurgy process, on the microstructure and mechanical properties of β-type Ti–25Nb–25Zr alloy (TNZ) for biomedical applications. The TNZ alloy was fabricated from a mixture of TiH_2 with elemental Ti, Nb and Zr powders (MM-Process) and as-received pre-alloyed Ti–25Nb–25Zr powder (IP-Process). The main conclusions drawn from the results obtained are as follows:

(1) Through mechanical milling of a mixture of TiH_2 with pure Ti, Nb and Zr powders, powder particle size could be reduced from several micron sizes to the sub-micron sizes wherein all the elements are uniformly distributed.
(2) After spark plasma sintering (at 1273 K), the chemically homogeneous TNZ compacts with primarily β-phase was obtained from a mechanically milled powder of TiH_2 with pure Ti, Nb, and Zr powders, as well as pre-alloyed Ti–25Nb–25Zr powders.
(3) The grain size of the TNZ compact, prepared from as-received pre-alloyed powder, was significantly larger

(800 μm) as compared to that prepared from TiH_2 and elemental powders (4.6 μm).

(4) The TNZ compact fabricated by TiH_2 and elemental powders exhibited significantly higher strength and optimum ductility (1140 MPa and 11%) as compared to that prepared by pre-alloyed powder (631 MPa and 27%).

The fabricated Ti–25Nb–25Zr alloy, using TiH_2, seems to be not less prone to hydrogen embrittlement but even profits from its presence in a limited amount. The cost-effective powder metallurgy processing of TiH_2 with elemental Ti, Nb and Zr powders demonstrated the capability to obtain β-phase TNZ alloy with suitable biomedical properties in terms of outstanding mechanical properties with fine-grained microstructure.

Acknowledgment

This work was supported by Grants-in-Aid for "Scientific Research on Innovative Areas on High Entropy Alloys" through the grant number 18H05455, and JSPS KAKENHI Grant Number JP18K18962.

REFERENCES

1) Y. Fukuzumi, T. Wada and H. Kato: *Interface Oral Health Science 2014*, ed. by K. Sasaki, O. Suzuki and N. Takahashi, (Springer, Berlin, 2015) pp. 93–101.
2) M. Niinomi: Sci. Technol. Adv. Mater. **4** (2003) 445–454.
3) J.Y. Rho, T.Y. Tsui and G.M. Pharr: Biomaterials **18** (1997) 1325–1330.
4) H.C. Hsu, S.C. Wu, Y.C. Sung and W.F. Ho: J. Alloy. Compd. **488** (2009) 279–283.
5) M.V. Oliveira, L.C. Pereira and C.A.A. Cairo: Mater. Res. **5** (2002) 269–273.
6) E.D. Spoerke, N.G. Murray, H. Li, L.C. Brinson, D.C. Dunand and S.I. Stupp: Acta Biomater. **1** (2005) 523–533.
7) H. Tobe, H.Y. Kim and S. Miyazaki: Mater. Trans. **50** (2009) 2721–2725.
8) T. Yu, H. Yin, Y. Zhou, Y. Wang, H. Zhu and D. Wang: Mater. Trans. **58** (2017) 326–330.
9) S. Kobayashi, S. Nakagawa, K. Nakai and Y. Ohmori: Mater. Trans. **43** (2002) 2956–2963.
10) J.H. Chang, J.F. Liu, Y.S. Sun, C.P. Wu, H.H. Huang and Y. Han: J. Alloy. Compd. **707** (2017) 220–226.
11) S.K. Vajpai, B. Sharma, M. Ota and K. Ameyama: Mater. Sci. Eng. A **736** (2018) 323–328.
12) F. Mompiou, D. Tingaud, Y. Chang, B. Gault and G. Dirras: Acta Mater. **161** (2018) 420–430.
13) G. Dirras, D. Ueda, A. Hocini, D. Tingaud and K. Ameyama: Scr. Mater. **138** (2017) 44–47.
14) J. Zhang, F. Sun, Y. Hao, N. Gozdecki, E. Lebrun, P. Vermaut, R. Portier, T. Gloriant, P. Laheurte and F. Prima: Mater. Sci. Eng. A **563** (2013) 78–85.
15) R.B. Osman and M.V. Swain: Materials **8** (2015) 932–958.
16) S.K. Vajpai, C. Sawangrat, O. Yamaguchi, O.P. Ciuca and K. Ameyama: Mater. Sci. Eng. C **58** (2016) 1008–1015.
17) V.A.R. Henriques, E.T. Galvani, S.L.G. Petroni, M.S.M. Paula and T.G. Lemos: J. Mater. Sci. **45** (2010) 5844–5850.
18) B. Sharma, S.K. Vajpai and K. Ameyama: J. Alloy. Compd. **656** (2016) 978–986.
19) B. Sharma, S.K. Vajpai and K. Ameyama: J. Alloy. Compd. **683** (2016) 51–55.
20) B. Sharma, S.K. Vajpai and K. Ameyama: Metals **8** (2018) 516.
21) I.M. Robertson and G.B. Schaffer: Powder Metall. **53** (2010) 12–19.
22) D.W. Lee, H.S. Lee, J.H. Park, S.M. Shin and J.P. Wang: Procedia Manuf. **2** (2015) 550–557.
23) Y.N. Zhang, C.M. Wang, Y.G. Zhang, P. Cheng, Y.H. Wei, S.F. Xiao and Y.G. Chen: Mater. Manuf. Process. **32** (2017) 1869–1873.
24) J.-M. Oh, K.-H. Heo, W.-B. Kim, G.-S. Choi and J.-W. Lim: Mater. Trans. **54** (2013) 119–121.
25) O.M. Ivasishin, D. Eylon, V.I. Bondarchuk and D.G. Savvakin: Defect Diffus. Forum **277** (2008) 177–185.
26) D.H. Kohn and P. Ducheyne: J. Mater. Sci. **26** (1991) 534–544.
27) K.R. Morasch and D.F. Bahr: Scr. Mater. **45** (2001) 839–845.
28) S.G. Schneider, C.A. Nunes, S.O. Rogero, O.Z. Higa and J.C. Bressiani: Biomecanica **8**(1) (2000) 84–87.
29) T. Lee, Y.-U. Heo and C.S. Lee: Scr. Mater. **69** (2013) 785–788.
30) G. Dirras, L. Lilensten, P. Djemia, M.L. Brocq, D. Tingaud, J.P. Couzinie, L. Perriere, T. Chauveau and I. Guillot: Mater. Sci. Eng. A **654** (2016) 30–38.
31) D. Khang, J. Lu, C. Yao, K.M. Haberstroh and T.J. Webster: Biomaterials **29** (2008) 970–983.
32) M.A. Hussein, C. Suryanarayana and N. Al-Aqeeli: Mater. Des. **87** (2015) 693–700.